AFRL-RX-WP-TR-2019-0235

TOTIPOTENT SYNTHETIC MATERIALS

S. Andrew Sarles and Scott Lenaghan

University of Tennessee Knoxville (UTK)

Donald Leo and Eric Freeman

University of Georgia (UGA)

26 JULY 2019
Final Report

AIR FORCE RESEARCH LABORATORY
MATERIALS AND MANUFACTURING DIRECTORATE
WRIGHT-PATTERSON AIR FORCE BASE, OH 45433-7750
AIR FORCE MATERIEL COMMAND
UNITED STATES AIR FORCE

NOTICE AND SIGNATURE PAGE

Using Government drawings, specifications, or other data included in this document for any purpose other than Government procurement does not in any way obligate the U.S. Government. The fact that the Government formulated or supplied the drawings, specifications, or other data does not license the holder or any other person or corporation; or convey any rights or permission to manufacture, use, or sell any patented invention that may relate to them.

This report is the result of contracted fundamental research deemed exempt from public affairs security and policy review in accordance with SAF/AQR memorandum dated 10 Dec 08 and AFRL/CA policy clarification memorandum dated 16 Jan 09. This report is available to the general public, including foreign nationals. Copies may be obtained from the Defense Technical Information Center (DTIC) (http://www.dtic.mil).

AFRL-RX-WP-TR-2019-0235 HAS BEEN REVIEWED AND IS APPROVED FOR PUBLICATION IN ACCORDANCE WITH ASSIGNED DISTRIBUTION STATEMENT.

//SIGNATURE//	//SIGNATURE//
THOMAS COOPER	CHRISTOPHER BREWER
Work Unit Manager	Branch Chief
Photonic Materials Branch	Photonic Materials Branch
Functional Materials Division	Functional Materials Division
Materials and Manufacturing Directorate	Materials and Manufacturing Directorate

This report is published in the interest of scientific and technical information exchange, and its publication does not constitute the Government's approval or disapproval of its ideas or findings.

REPORT DOCUMENTATION PAGE

Form Approved
OMB No. 0704-0188

1. REPORT DATE *(DD-MM-YY)*	2. REPORT TYPE	3. DATES COVERED *(From - To)*
26 July 2019	Final	27 June 2018– 26 June 2019

4. TITLE AND SUBTITLE
Totipotent Synthetic Materialst

5a. CONTRACT NUMBER
FA8650-18-1-7870

5b. GRANT NUMBER

5c. PROGRAM ELEMENT NUMBER
62101F

6. AUTHOR(S)
S. Andrew Sarles and Scott Lenaghan - University of Tennessee Knoxville (UTK)
Donald Leo and Eric Freeman - University of Georgia (UGA)

5d. PROJECT NUMBER
DARPA

5e. TASK NUMBER

5f. WORK UNIT NUMBER
X1HZ

7. PERFORMING ORGANIZATION NAME(S) AND ADDRESS(ES)

University of Tennessee Knoxville (UTK)
1331 Circle Park Dr.
Knoxville, TN 37996

University of Georgia (UGA)
1331 Circle Park Dr.
Knoxville, TN 37996

8. PERFORMING ORGANIZATION REPORT NUMBER

9. SPONSORING/MONITORING AGENCY NAME(S) AND ADDRESS(ES)

Air Force Research Laboratory
Materials and Manufacturing Directorate
WPAFB, OH 45433-7750
Air Force Materiel Command
United States Air Force

Defense Advanced Research Projects Agency (DARPA)
3701 North Fairfax Drive
Arlington VA 22203-1714

10. SPONSORING/MONITORING AGENCY ACRONYM(S)
AFRL/RXAP

11. SPONSORING/MONITORING AGENCY REPORT NUMBER(S)
AFRL-RX-WP-TR-2019-0235

12. DISTRIBUTION/AVAILABILITY STATEMENT
DISTRIBUTION STATEMENT A. Approved for Public release: Distribution is unlimited.

13. SUPPLEMENTARY NOTES
Report contains color.

14. ABSTRACT *(Maximum 200 words)*
This report summarizes the research progress made on a 1-yr seedling project focused on demonstrating proof of concept that stimuli-triggered, cell-free protein synthesis using engineered DNA and machinery from bacterial cells in synthetic compartmentalized materials can provide a path toward a diverse class of materials that can adapt their compositions and properties in ways similar to totipotent plant cells. Our unique approach incorporated stimuli-sensitive riboswitches and cell-free machinery in cell-inspired compartments separated by lipid membranes. The project was successful in demonstrating that multiple kinds of stimuli-responsive riboswitches can function, independently and orthogonally from other stimuli, in the same compartments of the material. Further, our plasmid designs demonstrate the modularity of this approach in creating new types of adaptive, functional materials.

15. SUBJECT TERMS
Cell-free protein synthesis, totipotent, riboswitches, compartmentalized materials, biological materials, responsive materials

16. SECURITY CLASSIFICATION OF:			17. LIMITATION OF ABSTRACT:	18. NUMBER OF PAGES	19a. NAME OF RESPONSIBLE PERSON (Monitor)
a. REPORT	b. ABSTRACT	c. THIS PAGE			Thomas Cooper
Unclassified	Unclassified	Unclassified	SAR	28	19b. TELEPHONE NUMBER *(Include Area Code)* (937) 255-9620

Standard Form 298 (Rev. 8-98)
Prescribed by ANSI Std. Z39-18

TABLE OF CONTENTS

LIST OF FIGURES

Section **Page**

LIST OF TABLES

Section **Page**

1.0 SUMMARY

This project aimed to demonstrate proof-of-concept that merging state-of-the-art synthetic cell-free biology within bio-inspired compartmentalized materials provides a new path towards developing synthetic materials that can "learn" their properties in response to physical cues—similar to the *totipotency* of plant cells which enables external stimuli to direct differentiation into various tissue types. To meet this goal, our team conducted parallel studies in model test cells and single building block compartments to: 1) design stimuli-responsive synthetic biology reaction cassettes for generating functional proteins and thereby changing the properties of the material; and 2) assess the sensitivities of these reactions to stimuli and the resulting material property changes in response to stimulus exposure. Two examples of differentiated materials were pursued: one that exhibits an increase in mechanical stiffness, due to cell-free production of structural protein actin triggered by heat, and a second, which exhibits an increase in ionic conductivity upon selective production of alpha-hemolysin membrane pores in response to a chemical trigger. The seedling project had 3 aims.

Aim 1: Develop orthogonal, stimuli-sensitive cell-free reaction schemes for producing different proteins in response to two different external signals. The *objective* and *primary deliverable* of Aim 1 was to develop and characterize, outside of a material compartment, two cell-free reaction schemes capable of sensing separate stimuli (temperature change or a molecular trigger) and responding with the production of different proteins (actin and alpha hemolysin).

Aim 2: Demonstrate and assess change in mechanical properties of compartmentalized material caused by expression of actin. The *objectives* and *primary deliverable* of Aim 2 were to demonstrate in compartments that this process can be induced by a temperature-sensitive RNA thermometer and assess changes in material stiffness caused by actin generation/polymerization.

Aim 3: Demonstrate and assess change in transport properties of compartmentalized material caused by expression of alpha-hemolysin. The *objectives* and *primary deliverables* of Aim 3 were to demonstrate within a compartmentalized material embodiment and assess the extent to which the material's ionic conductivity can be increased by the presence of an external molecular trigger, which causes an RNA thermometer to initiate membrane-channel production.

2.0 INTRODUCTION

The overarching goal of this seedling project is to integrate cell-free synthetic biology machinery within a tissue-inspired compartmentalized synthetic material to enable the production of proteins from genetic code (i.e. DNA) and thereby a change of material properties in response to external stimuli. **Error! Not a valid bookmark self-reference.** illustrates key concepts and terminology explored in our project.

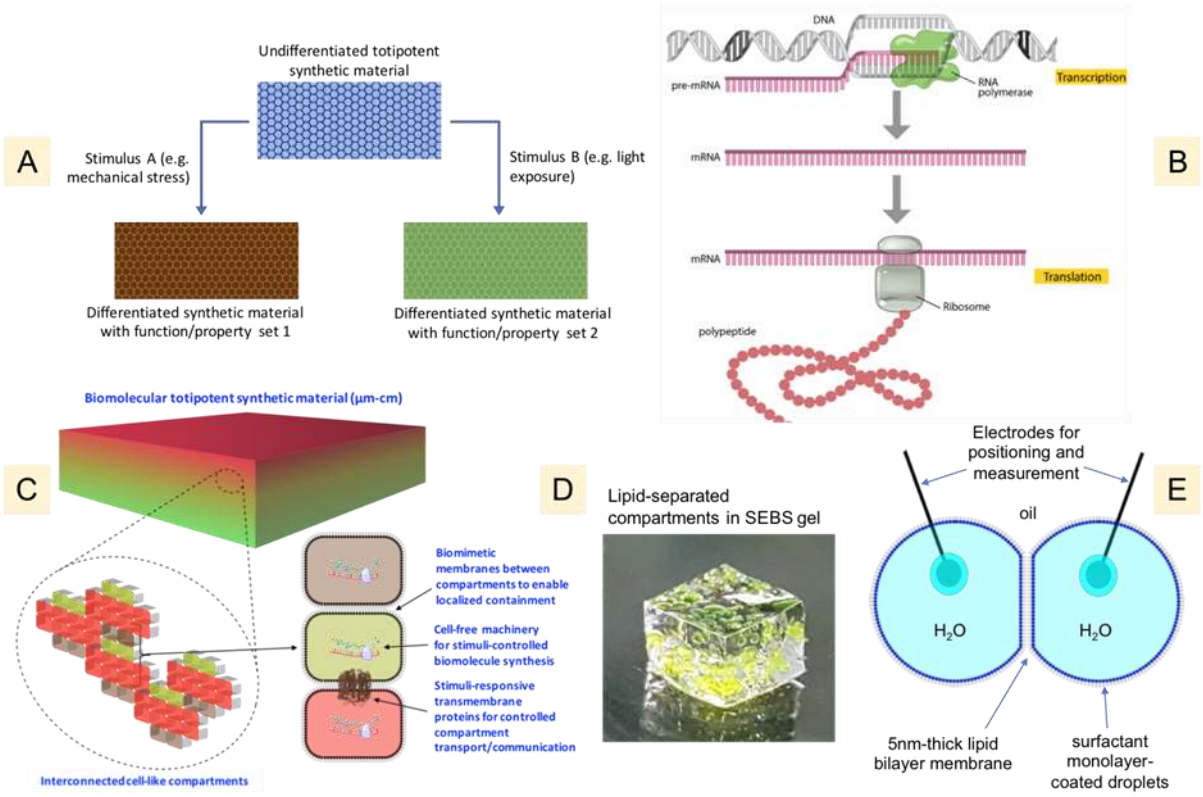

Figure 1. Synthetic totipotent material.

(A) Illustration of an undifferentiated material that contains genetic information and stimuli-responsive machinery which enables it to be transformed into different materials with disparate compositions and properties.

(B) Schematic illustrating the two-stage process for creating proteins from genetic information. In step 1, DNA (e.g. plasmids) are transcribed into messenger ribonucleic acids (mRNA) via RNA polymerase enzymes. In step 2, ribosomes join mRNA with corresponding transfer RNA (tRNA) that carry amino acids to translate polypeptide structures. Performing these reactions outside of a cell is known as cell-free (or in vitro) transcription (TX) and translation (TL)). Riboswitches are portions of the mRNA that undergo conformational changes that either turn ON or OFF translation of sections of the genes of interest that code for specific protein products. In this project, we will explore multiple riboswitch designs to enable external stimuli to dictate cell-free TX/TL reactions and thereby control the type of proteins produced.

(C) A generalized embodiment of the envisioned material system enabled by this research. The hierarchical material consists of many cell-like compartments contained within an exterior solid matrix. Each compartment may contain cell-free machinery (nucleic acids, amino acids, RNA polymerase, tRNA, ATP, etc.) for generating RNA or proteins in situ as well as other biomolecules (e.g. amino acids, nucleotides, phospholipids), carbohydrates, ions, etc. As shown, the network of embedded compartments

can be interconnected via biomimetic membranes or they can be isolated compartments that interact with their surroundings and other compartments via signal transduction and/or multiphase transport. (D) An image of one embodiment of a 3D compartmentalized material assembled at UGA achieved by printing lipid-encased aqueous compartments within an oil-based polymeric gel (organogel). (E) Two droplets connected by a droplet-interface bilayer (DIB) serve as the building blocks and model unit cell of our compartmentalized material. We will use variations of this two-volume assembly to characterize the effects of cell-free protein synthesis (CFPS) on individual compartment properties.

3.0 RESULTS AND DISCUSSION OF RESEARCH SCOPE DURING Q3-Q4[†]

3.1 Complete the assembly of stimuli-responsive riboswitches riboswitches and quantify their ability to produce proteins.

During Q3-Q4, we successfully constructed a plasmid containing the *pThermeleon* riboswitch that enables temperature-dependent production of red fluorescent protein (RFP, mCherry variant) and actin. RFP is produced at temperatures between ~38-43, while actin is produced only near 45C. We performed fluorescence-based microplate assays to confirm temperature dependence of the riboswitch, and used Bradford assays to quantify total protein production versus temperature (**Error! Reference source not found.**). Also, we combined *pThermeleon* with *JF001A*, a separate, chemically-triggered riboswitch developed in Q2 that encodes for GFP and alpha-hemolysin (aHL) membrane proteins, into same aqueous cell-free extract (CFE) environment to explore their orthogonal stimuli-responsive outputs. These studies confirmed that JF001A does not show GFP (or aHL) production across temperatures from 30-45C (Figure 4). Instead, GFP and aHL production occurs only in response to the chemical trigger theophylline (TP), which can enter compartments from the surrounding oil phase (**Error! Reference source not found.**). Meanwhile, exposure of *pThermeleon* to TP does not yield RFP or actin (**Error! Reference source not found.**).

When combined with our prior progress, these results represent successful completions of Task 1, including Milestones 1.1-1.3, and demonstrate that multiple stimuli-responsive riboswitches can be housed in similar compartments of a material and conduct, without interference, separate reaction schemes. This capability to house multiple functionalities/genes within regions of a material is a hallmark of our concept for *synthetic totipotency*.

3.2 Demonstrate temperature-induced in situ actin production and subsequent polymerization results in solidification of aqueous compartments.

Using micropipette aspiration, we qualitatively assessed changes in mechanical properties of the aqueous compartments via polymerization of actin monomers, originating from either a commercial kit or synthesized *in situ* using the temperature-sensitive *pThermeleon* riboswitch. These experiments showed that polymerization of actin within the compartments changes the rheological and optical properties of the volume, which caused it to retain its shape and overall volume upon negative pressure aspiration (**Error! Reference source not found.**). This technique also revealed that the heating of aqueous volumes containing CFE beyond ~35C resulted in the formation of a "skin" at the surface of the droplet, independent from actin. Negative pressures applied to these volumes resulted in a collapse of the volume, i.e. similar to a deflating balloon.

These results demonstrate successfully the polymerization actin produced by a cell-free, stimuli-triggered reaction alters the mechanical properties of the material compartments. However, measurements of nominal change in compartment stiffness were not obtained, and the effects on material stiffness in higher order assemblies in solidified hydrophobic matrices.

[†] This report includes some central information also provided in the Q1 and Q2 reports to aid the reader in understanding the broader goals of the project.

3.3 Demonstrate increased ion conductance of interfacial membranes through production of aHL via TP-triggered JF001A riboswitch.

Producing aHL increases the permeability of networks of membrane-separated compartments due to formation of membrane-spanning nanopores, as we demonstrated with pre-synthetized aHL added to compartments during Q1-Q2. In Q3-Q4, we carried out TP-triggered aHL reactions and used electrical measurements to assess increases in intra-membrane conductance. These experiments included: 1) measurements on membranes separating compartments containing the products of these reactions (incubated for 18 hours ahead of membrane formation) (**Error! Reference source not found.**); and 2) in situ measurements made across membranes between droplets undergoing cell-free reactions (**Error! Reference source not found.**). In both cases, we observed higher membrane conductance when reactions contained TP. However, quantitative assessments of the number of channels inserting into the membrane over time was not successful due to increased membrane disruption/permeability caused by CFE alone.

4.0 ASSESSMENTS OF FEASIBILITY AND OPPORTUNITIES

Inspired by the total genetic potential (*totipotency*) of plants, this 1-year seedling project aimed to show that a synthetic biology route combined with a cell-inspired compartmentalized material system can enable the development of materials that "learn/evolve" their compositions and behaviors through in situ production of proteins, which alter the properties of the system.

4.1 Clear Successes

Task 1: Riboswitch-containing plasmids and orthogonal functionality demonstrated successful stimuli-responsive pathways for controlling protein production, even using non-purified CFE, which is significantly cheaper than commercially-available purified systems (PURE, etc.). In addition to each riboswitch responding positively to their own stimuli, they each showed strong insensitivity to the other's stimulus. For example, the chemically-triggered riboswitch (*JF001A*) was not influenced by changes in temperature from 30-45, while the heat-sensitive riboswitch (*pThermeleon*) was unaffected by theophylline. This allows for colocalization of multiple plasmids (riboswitches and their corresponding gene(s) of interest) in materials, and provides strong momentum for continuing our pursuit to genetically encode properties and functions in materials.

4.2 Remaining Challenges

The primary challenges encountered in this system occurred upon integration of the CFE and plasmids into our multiphase (oil/water/amphiphile) material system.

First, our experiments revealed that crude CFE from *E. coli* interferes with membrane stability and increases bilayer permeability. This likely indicates some fraction of amphiphilic species contained in the CFE that associate with the lipid monolayer and bilayers, thereby disrupting packing of lipids. This limits the ability for intra-compartment membranes to remain impermeant to small molecules, including ions. Electrical measurements of membrane conductivity and rupture potentials are proof of this effect, and similar effects were also observed when pre-synthesized actin monomers are incorporated into the compartments. These non-specific increases in permeability complicated our ability to distinguish increases in membrane conductivity due to successfully TP-triggered aHL assembly/insertion versus non-specific membrane leakage. Lipid disruption also impacts the ability for the membrane to stabilize the organization and maintain desired compartmentalization of species in a higher-order material assembly (such as shown in Figure 1C). This prevents successful study of distributed sensing and protein production responses within assemblies of >2 compartments, and integration of compartments into solidified organic matrices (as shown in Figure 1D).

Second, we learned that mixtures of lipids and CFE are prone to gelation induced by heating. Our aspiration experiments (**Error! Reference source not found.**) show that non-specific gelation predominantly occurs near the oil-water interface at the surface of the droplets, which results in the formation of a "skin" surrounding the droplet. The rest of the compartment appears to remain in a liquid state. It is not clear what the specific composition(s) of these skins are. While we were able to confirm that actin polymerization results in solidification of a larger percentage of the compartment volume (i.e., the whole droplet appears to solidify), a nonspecific solidification near the interface may further disrupt the lipid organization of the membrane.

Removing the CFE eliminated the “skin” formation upon heating, though it is not clear if a purified CFE mixture could eliminate these effects.

Therefore, it remains a challenge to integrate CFE into amphiphile (lipid) stabilized compartmentalized materials without disrupting the assembly and desired barrier properties of the interface membranes, including at elevated temperatures (25-45) commonly required for protein translation.

4.3 New opportunities identified for leveraging momentum of Phase I seedling

A defining aspect of our vision to develop stimuli-responsive materials that leverage cell-free synthetic biology is to compartmentalize the reaction products (RNA, proteins) such these products can alter properties of the material in a temporally and spatially controlled fashion. Complete isolation enables distinct chemistries to occur in different regions; however, the ability to share species and communicate events has the potential to realize collective responses and amplified transformations across many compartments.

This project revealed limitations of employing amphiphile stabilized compartments. Thus, in continued efforts (possibly a Phase II seedling project), we propose to leverage a recently-demonstrated approach that localizes DNA to microgels[1, 2]. **Error! Reference source not found.**A shows the general concept of this system, where cross-linked hydrogels that either encapsulate or covalently bound various machinery are contained in a purely aqueous environment. The gel microspheres can be made simply using emulsion techniques or via microfluidic dispensing, and they can also be further encapsulated/isolated in oil-surrounded volumes as shown in **Error! Reference source not found.**B if desired. The gel chemistries and linkages vary slightly in these two works, but both are able to compartmentalize the reactions (not necessarily all reactants, machinery, RNA, or proteins, as some can still diffuse in and out) without needing lipid monolayers or membranes, or oil. Moreover, the reactions can be subdivided by compartment: some spheres can be for transcription of RNA/riboswitches and some for translation of proteins, where diffusion of products/reactants through their shared aqueous media allow them to communicate. As both of these studies used expensive purified cell-free expression systems, there is an opportunity to broaden the impact of these works by studying cell-free expression.

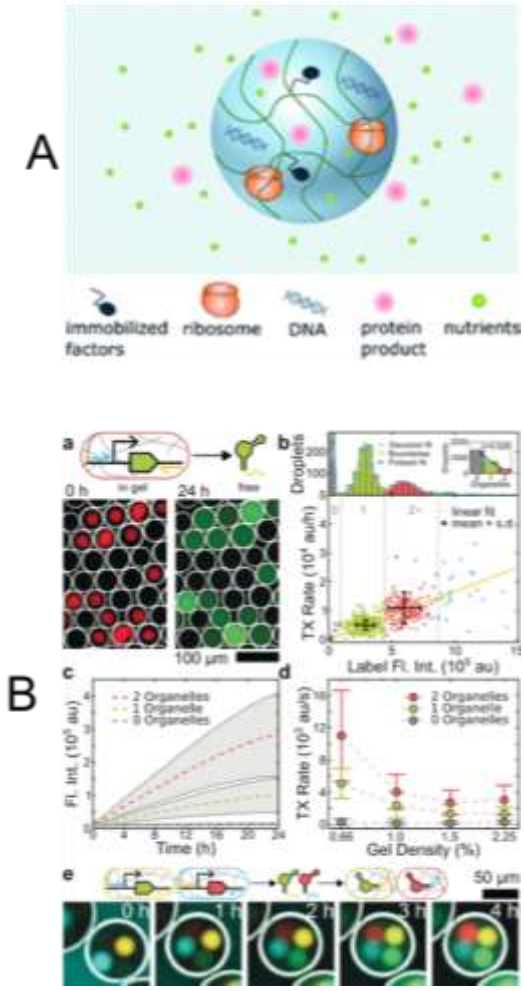

Figure 2. Proposed gel-based approach; (A) to contain and spatially-organize cell-free reactions (B) for building hierarchical totipotent materials.

The use of gels as the compartment framework may change what we could demonstrate regarding adaptive properties (maybe not mechanical stiffening via actin polymerization, and likely not increased communication or conductance via aHL pore formation). However, a cross-linked compartment building block provides other key advantages:

- Using gel-stabilized particles, we could precisely print/layer them into larger 3D matrices to create hierarchical adaptive materials, including those that can convert and store energy, process chemical information, and serve as portable biomolecular factories. This could enable generations of modular, multi-functional, wearable, implantable, and, possibly, edible materials whose compositions and functions (or dietary value) depend on applied stimuli and embedded totipotency.
- Gel materials, compared to amphiphile-stabilized compartments, could allow for more robust packaging strategies, for example to enable smart packaging that senses biological agents/contamination in food or water, or on a warfighter's person.

5.0 CUMULATIVE PROGRESS TOWARD MILESTONES

5.1 Task 1.1 Develop and Characterize Scheme 1 Synthetic Biology Cassettes for Sensing Temperature Changes and Producing Actin and Fluorescent Proteins

5.1.1 Milestone 1.1.1 Design/Synthesize Plasmids for 3 Variants of Scheme 1, Each of which Includes Necessary Expression Promoter, RNA, and Genes of Interest Sequences.

During Q1, thermal switches (*pCali2* and *pThermeleon*) designed for dual responsive protein translation of RFP and GFP (i.e. two different genes of interest controlled by temperature) were constructed by Addgene. Recall that *pCali2* exhibited high levels of GFP expression from 38-40°C, with RFP reaching a maximum between 40-45°C. For *pThermeleon*, the switch was more specific, with a maximum level of GFP produced at 45°C, with little RFP expression, compared to very high levels of RFP at 43°C with relatively no GFP production.

During Q3-Q4, we cloned in-house a new plasmid variant (**Error! Reference source not found.**A) that uses a *pThermeleon* riboswitch and includes genes of interest for encoding RFP (mCherry) and actin, the latter which replaces GFP in the prior variant (Figure 2 of Q2 report). As labeled in **Error! Reference source not found.**A, the gene of interest for actin (grey portion) is inserted into the vector at the prior starting location of GFP (mWasabi). The difference in the lengths of these genes results in a non-functional fraction of the mWasabi gene to remain in the 9435 base pair-long vector.

5.1.2 Milestone 1.1.2 Confirm Temperature-Sensitive RNA Thermometer Functionality, and Quantify RFP Protein Production Kinetics and Sensitivity.

After synthesis, we separately incubated mixtures of CFE and this plasmid at varying temperatures for fixed durations (**Error! Reference source not found.**B) and then measured the RFP fluorescence intensity (587 nm excitation, 610 nm emission) using a microplate reader. **Error! Reference source not found.**C shows that RFP fluorescent intensity, which is proportional to the concentration of RFP produced via cell-free protein expression, increases with incubation temperatures between 36-43C. For comparison, **Error! Reference source not found.**D compares the fluorescence intensities of both RFP and GFP measured on the prior plasmid containing the same riboswitch. In both, RFP intensity drops substantially at 45C, indicating far less RFP translation at this temperature, while GFP (i.e. the 2nd gene of interest) is expressed only at temperatures above 43C. The agreement between the RFP data in **Error! Reference source not found.** C, D indicate the newly cloned plasmid maintains the same temperature-dependence selectivity for *in vitro* translation. Newly cloned plasmid maintains the same temperature-dependence selectivity for *in vitro* translation.

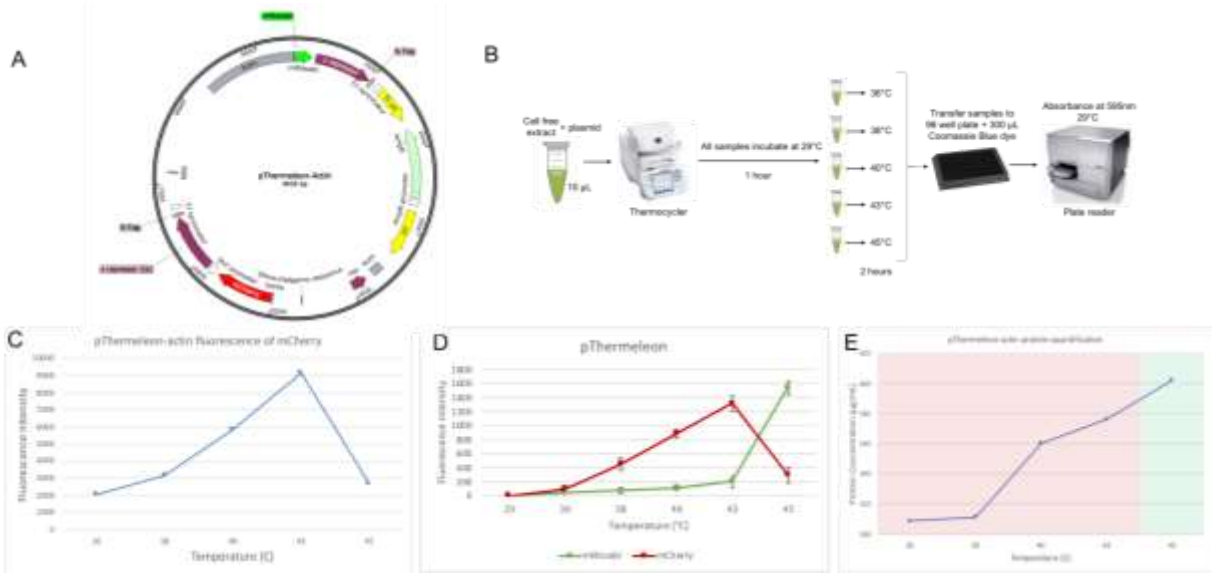

Figure 3. Synthesis and assessment of temperature-sensitive protein production.

(A) Plasmid DNA design for a dual-temperature pThermeleon riboswitch that includes mCherry (RFP) and actin genes of interest.
(B) Experimental scheme for incubation and microplate-based measurement of protein production.
(C) Nominal RFP fluorescence intensity versus incubation temperature assessed using plasmid shown in A.
(D) Nominal RFP and GFP intensities versus incubation temperature measured during Q1 on prior plasmid variant.
(E) Total protein concentration versus incubation temperature obtained from plasmid shown in (A).

5.1.3 Milestone 1.1.3 Quantify Actin Protein Production and Sensitivity to Temperature.

We used a Bradford assay to quantify total protein concentration versus incubation temperature. **Error! Reference source not found.**E illustrates that the total protein concentration rises above the baseline level (generated by proteins present in the CFE) at temperatures above 38C. The continued rise in total protein concentration from 43C to 45C, along with the drop in RFP fluorescence intensity at 45C, indicates actin protein production occurring above 43C. This graph indicates that ~70 µg/ml (above the baseline) of RFP is produced at 43C and nearly 100 µg/ml of actin is produced at 45C.

5.2 Task 1.2 Develop and Characterize Scheme 2 Cassettes for Sensing Theophylline and Producing Alpha Hemolysin and FP Proteins

5.2.1 Milestone 1.2.3 Quantify aHL Protein Production and Sensitivity to TP.

During Q2, we cloned in-house plasmid DNA containing a theophylline (TP)-sensitive riboswitch (*JF001A*) that encodes for expression of alpha hemolysin (aHL) membrane proteins and GFP. After cloning, the construct was sequence validated and demonstrated to be the correct construct. In Q3-Q4, we performed microplate assays with the same plasmid to demonstrate sensitivity to varying concentrations of TP and explore delivery of TP from the surrounding oil phase, a necessity for enabling material learning from a sensed chemical.

Error! Reference source not found.A shows the change in GFP fluorescence intensity versus time for varying concentrations of the trigger, TPA. As expected, the largest increase in GFP intensity (and thus GFP and aHL concentration) occur at the highest concentration (1.5 mM) of TPA (grey data). Removing the plasmid from the mix (yellow data), results in the least change and lowest nominal signal. Removing all TPA and including DNA (blue data) results in a small amount of fluorescence increasing, likely the result of non-specific riboswitch opening that enables some protein production. A ten-fold dilution of TPA (0.15 mM, orange data) results in a significantly higher amount of fluorescence indicating the minimum threshold of detection in this scheme is less than 0.15 mM. In comparison to the data in Figure 2C-E, these data show that TP-triggered aHL+GFP production via *JF001A* occurs much slower that production of RFP and actin using *pThermeleon*.

Error! Reference source not found.B shows the measured fluorescence intensity of a 4 µL aqueous mixture of CFE and buffer surrounded by 100 µL of oil (2:1 v:v hexadecane:AR20) in a 300 µL microplate well. Similar to **Error! Reference source not found.**A, we see that surrounding the CFE+DNA droplet with oil lacking the theophylline (TPB, an oil-soluble TP variant synthesized in-house during Q1-Q2) results in some non-specific protein translation (orange data). However, including TPB (3mM) in the oil results in significantly higher amounts of protein translation (grey data), where synthesis occurs at a maximal rate within the first 4 hours at 29C. This reaction rate is quicker than what was observed in **Error! Reference source not found.**A when TPA was included in the aqueous phase due to a higher concentration of trigger in the oil. This finding demonstrates that TPB can passively diffuse from the oil phase into the aqueous droplet where the riboswitch is located. The fact that we do not observe a significant delay or slower protein production suggests that transport of TPB is faster than protein translation within the droplet.

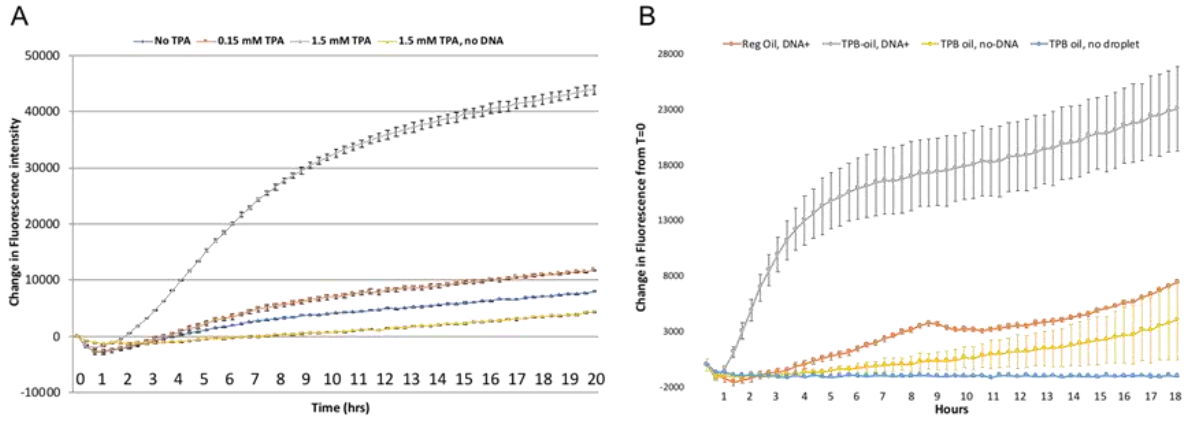

Figure 4. Theophylline-triggered protein production

(A) GFP fluorescence intensity versus time for varying concentrations of theophylline acetate (TPA).
(B) GFP fluorescence intensity versus time for varying oil compositions encasing the aqueous mixture. All reactions were performed at 29C.

5.3 Task 1.3 Examine Efficiency of Schemes 1 and 2 for Orthogonal Protein Production When They are Co-Located in the Same Medium

5.3.1 Milestone 1.3.1 Quantify Actin and aHL Protein Production and Their Corresponding Sensitivities to Theophylline and Temperature.

In Q3-Q4, we assessed the responses of both plasmids to both temperature and theophylline. These measurements were performed with both plasmids and CFE collocated in the same aqueous volume, chosen to mimic the mutual incorporation into the same compartments of a material. **Error! Reference source not found.**A shows the variations in RFP (from *pThermeleon*) and GFP (from *JF001A*) versus incubation temperature. Similar to the data in Figure 2, the RFP response shows peak RFP production at 43C, followed by a sharp drop at 45C, where actin is alternatively produced. In contrast, little to no GFP is produced across the entire temperature range (during the 2-hour incubation scheme, shown in **Error! Reference source not found.**B). Repeating this experiment with 1 mM theophylline present yielded no detectable differences in RFP production versus temperature (not shown). Furthermore, production of GFP and aHL from JF001A was found to increase slightly with increasing temperature (**Error! Reference source not found.**B), suggesting some protein is produced in the 2-hour incubation and that kinetics of GFP and aHL production likely quicken at temperatures > 30C.

A second experiment was the conducted to assess the response of each plasmid to theophylline. Figure 4C shows the fluorescence measured for aqueous samples containing CFE, both plasmids, and either 0 or 1.5 mM TPA. The excitation and emission ranges enable capturing emission from both RFP and GFP. During the first 10 hours at a temperature of 30C (below that required to activate RFP or actin production), the samples containing TPA (orange data) produced GFP and aHL. The samples were then held at 43C for an additional 10 hours. Here, we see the samples without TP (blue data) now producing fluorescent protein (RFP). The samples that also contained TPA showed a continual rise in protein production, however it is unknown how much of this is GFP versus RFP.

Collectively, these results show strongly that the two different plasmids can exist in the same compartments of a material without inhibiting one another.

5.4 Task 2.1 Determine the Effects of CFE Machinery on Material Compartments

5.4.1 Milestone 2.1.1 Assess the Dynamic Interfacial Tension at Oil-Water Interface of a Compartment Containing CFE.

To improve monolayer formation and aid intercompartmental membrane stability, we studied the incorporation of lipids into both the aqueous and oil phases of our system. A DataPhysics OCA 25 video-based contact angle measuring device was again used to quantify the dynamic interfacial tension surrounding an aqueous pendant droplet submerged in oil.

Error! Reference source not found.A shows representative data from these measurements, conducted on aqueous volumes containing CFE an. For reference, the interfacial tension of a hexadecane-water interface is found to be 44 mN, while the equilibrium tension (reached in about 3 minutes) for DPhPC lipids (our standard lipid for interfacial membranes) is ~ 1 mN/m. These measurements revealed that the both the CFE and the require electrolyte buffer used for transcription and translation reactions reduce the interfacial tension of an oil-water interface even

in the absence of lipids; the buffer lowers the tension to c.a. 32 mN/m, while the full CFE brings the tension to c.a. 10 mN/m. Both processes reach steady state in c.a. 1-3 minutes.

Since Q2, we studied compartments assembled with lipids present in both liquid phases. The addition of lipids to both the aqueous and organic phases was found to increase the rate of monolayer formation, however it did not prevent the destabilizing effects of CFE contained within the droplet from disrupting the lipid packing and leading to shorter bilayer lifetimes, lower rupture potentials, and higher ionic permeability. The use of mineral oil in place of hexadecane oil was found to aid monolayer assembly too (**Error! Reference source not found.**B).

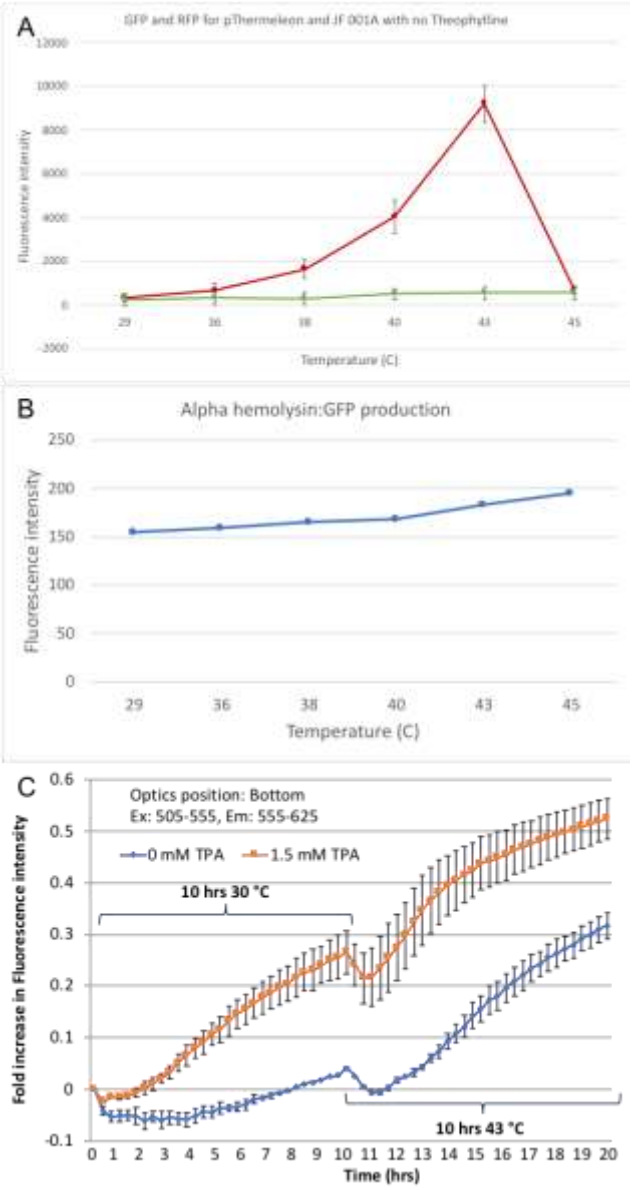

Figure 5. Orthogonal protein-production assessment.

(A) RFP (red) and GFP (green) fluorescence versus incubation temperature for samples containing both plasmids without theophylline.

(B) GFP fluorescence intensity versus incubation time for samples containing both plasmids and including 1mM TPA.
(C) Two-phase experiment on oil-encased 6 µL aqueous droplets containing both plasmids with and without TPA.

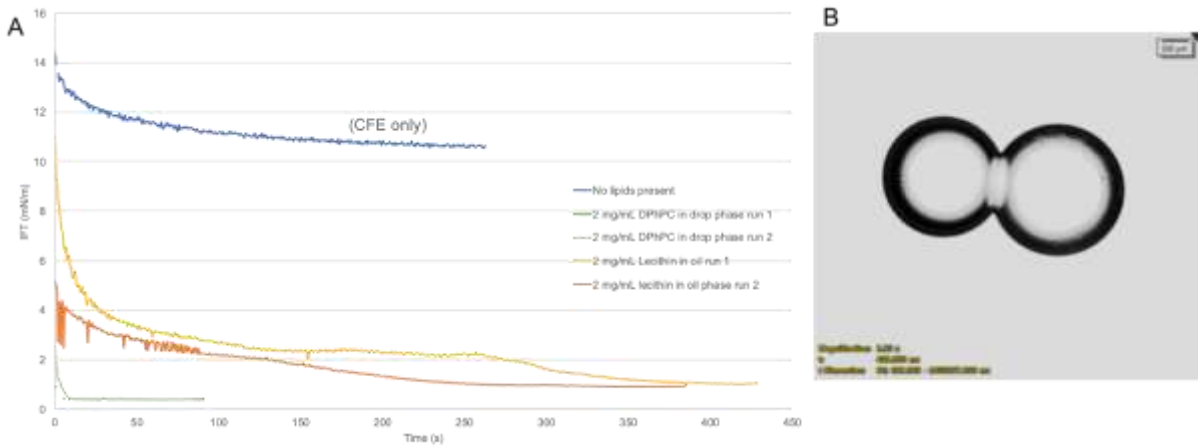

Figure 6: Effects of CFE on lipid monolayer assembling and membrane formation.

(A) Interfacial tension versus time obtained using a pendant drop goniometer device.
(B) Stable droplet interface bilayer formed in mineral oil between droplets containing DPhPC lipids and CFE.

5.5 Task 2.3 Analyze Theophylline Transport through an Oil-Based External Medium into Compartments for Triggering Material Response

5.5.1 Milestone 2.3 Determine the Diffusion Rate of Theophylline in SEBS Layer and the Resulting Sensing Time Lag in the Compartment.

Recall that in Q1 we established that TP and TPA chemical triggers have poor solubility in hexadecane and other alkane and silicone oils due to their inherent non-polarity. This caused them to remain as white crystalline solids when dispersed in oil. As a result, we hypothesized that, if sensed externally, TP and TPA would be poorly suited to diffuse through the oil phase to reach the aqueous volumes where triggering of reactions could occur. Then in Q2, we chemically synthesized and tested a novel tert-butyl ester form of the theophylline trigger—tert-butyl-theophyllinate (TPB). The chemical structure of synthesized TPB was confirmed via NMR. This additional group grafted to TP resulted in greater solubility in oil: synthesized TPB was found to be soluble in hexadecane at 1mM, and at 3mM in 1 mg/ml lecithin in 2:1 hexadecane:AR20 oil. Interestingly, we discovered that TPB results in higher amounts of HL protein production when using the *JF001A* plasmid developed during Q1.

In Q3-Q4, we examined the ability for TPB to enter the aqueous compartments from the oil phase. **Error! Reference source not found.**B shows that TPB passive diffuses from the surrounding oil to the interior of the aqueous droplets where it triggers production of GFP. While our measurements do not directly measure TPB transport, the rates of protein production are not significantly slower than in cases where TP is added to the aqueous phase. This demonstrated that TPB transport is relatively fast compared to *in vitro* protein production.

5.6 Task 2.4 Characterize Actin Network Structuring Within the Compartments, and Analyze the Change in Modulus of the Material in Response to Temperature

5.6.1 Milestone 2.4.2 Measurements of Compartment and Material-Level Stiffness Changes versus the Amount of Actin.

During Q2, we began using an aspiration-based method[3-5] to assess changes in compartment (droplet) stiffness. The technique uses a micro-forged glass capillary to aspirate the polymerized aqueous volume. The deformation caused by the applied negative pressure can be used to assess the surface tension, and areal elasticity of the compartment. The glass capillaries are treated with Sigmacote® to minimize droplet wetting (spreading) and a high-speed pressure clamp is used to draw a droplet into the capillary and hold it in place as the vacuum pressure is gradually increased. **Error! Reference source not found.** summarizes the types of qualitative compartment responses we observed. We initiated these studies on aqueous compartments containing pre-synthesized actin monomers and found that the polymerization of the volume resulted in either a solidified, yet smooth outer skin that caused the volume to deflate under suction (**Error! Reference source not found.**A, left) or apparent solidification of the entire volume, which became non-spherical and rough upon removal of excess fluid. In contrast, a non-polymerized volume remains spherical as it is suctioned into the capillary (**Error! Reference source not found.**B).

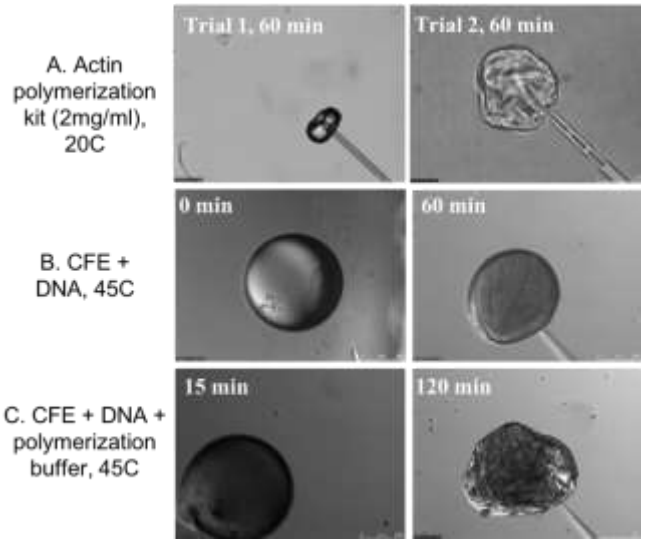

Figure 7. Aspiration-based assessment of changes in mechanical properties due to actin polymerization.

(A) Compartments loaded with a commercial actin polymerization kit and subjected to negative (suction) pressures. (B-C) Compartments containing CFE and *pThermeleon* plasmid to produce actin monomers at 45ºC.
(B) No polymerization buffer included.
(C) Polymerization buffer present to enable crosslinking of actin upon synthesis.

With this qualitative proof of changes in compartment mechanical properties we incorporated the necessary machinery to produce actin at 45C by triggering the *pThermeleon* riboswitch. **Error! Reference source not found.**B shows images of a compartment lacking the necessary polymerization buffer before and after 1 hour of protein production at 45C. Aspirating this volume revealed that the formation of solidified coating on the surface of the droplet, which wrinkled when suction was applied. Without the polymerization buffer, we saw no evidence of a solidified droplet core. Repeating this experiment with the polymerization included (**Error! Reference source not found.**C) caused a substantially different result in appearance and response to suction after 2 hours of reaction and polymerization at 45C. Specifically, we observed that the droplet became noticeably opaquer and the volume retained its overall shape upon aspiration (only excess liquid was removed by the capillary). This finding was repeatable, providing strong evidence of changes in mechanical properties enabled through stimuli-responsive protein production and polymerization. Quantitative measures of change in material properties were not obtained.

5.7 Task 3.1 Demonstrate and Assess Change in DIB Conductance upon Translation and Subsequent Membrane Insertion of aHL

5.7.1 Milestone 3.1.1 Demonstrate aHL Channel Insertion After Cell-Free Translation.

In Q1, we presented representative measurements of change in bilayer conductance versus time for membranes exposed to aHL purchased from Sigma Aldrich. In Q2, we replicated these measurements across multiple concentrations of alpha hemolysin protein added to the aqueous compartments on both sides of a droplet interface bilayer and confirmed that higher concentrations of aHL resulted in higher membrane conductance values. In Q3-Q4, we assessed changes in membrane conductance caused by TP-triggered synthesis of aHL. We first used the products of cell-free reactions (JF001A + CFE for 18 hours at 30C) to form droplet interface bilayers. **Error! Reference source not found.**A shows a representative current-voltage response obtained when the reaction was conducted in the absence of TPA and doped with additional DPhPC liposomes (2 mg/ml) in the aqueous phase to support bilayer stability. Here we see the membrane is highly resistive; current increases by only ~2 pA as the applied voltage increases from 20 to 60 mV. Including TPA in this reaction and again supplementing the droplet volumes with DPhPC liposomes results in membranes with higher conductances. **Error! Reference source not found.**B shows a representative measurement of current versus time in response to increasing voltages. Here we observe significantly higher changes in current as the voltage increases (the membrane also ruptured at 60mV, vs. 110 mV for the case without TPA). **Error! Reference source not found.**C compares the average current versus voltage for these two cases; the slope represents the conductance of the intercompartment membrane. Without TPA included in the reaction, bilayer conductance is c.a. 25 pS, versus c.a. 650 pS when TPA was included. This result is consistent with the possibility that aHL proteins produced during the reaction have inserted into the membrane.

Next, we performed experiments to examine the *in situ* synthesize of aHL as monitored by measurements of membrane conductance and dye leakage. Rather than using the products of cell-free reactions in the droplets, these experiments incorporate the necessary reactants, including the chemical trigger, to form aHL within the compartments. **Error! Reference source not found.**A shows an image of this two-droplet system, in which both droplets include CFE, DNA (JF001A), 0.75 mg/ml liposomes, and 1.5 mM TPA. The oil surrounding the droplets was

a 1:1 v:v mixture of hexadecane and AR20 and included 1 mg/ml DPhPC lipids to supplement monolayer formation. The right (donor) droplet contains 25 µg/ml fluorescein dye and is buffered to pH 6, while the left (acceptor) droplet is buffered to pH 7.9. This configuration is chosen to promote unidirectional, passive transport of fluorescein through the bilayer, in the presence of aHL channels. The entire system was then incubated at 29C for 8 hours during which the conductance of the membrane was continuously measured (Figure 9B-C) via the wire-type electrodes (see brightfield image) and transport of fluorescein was monitored intermittently via fluorescence imaging (Figure 9A).

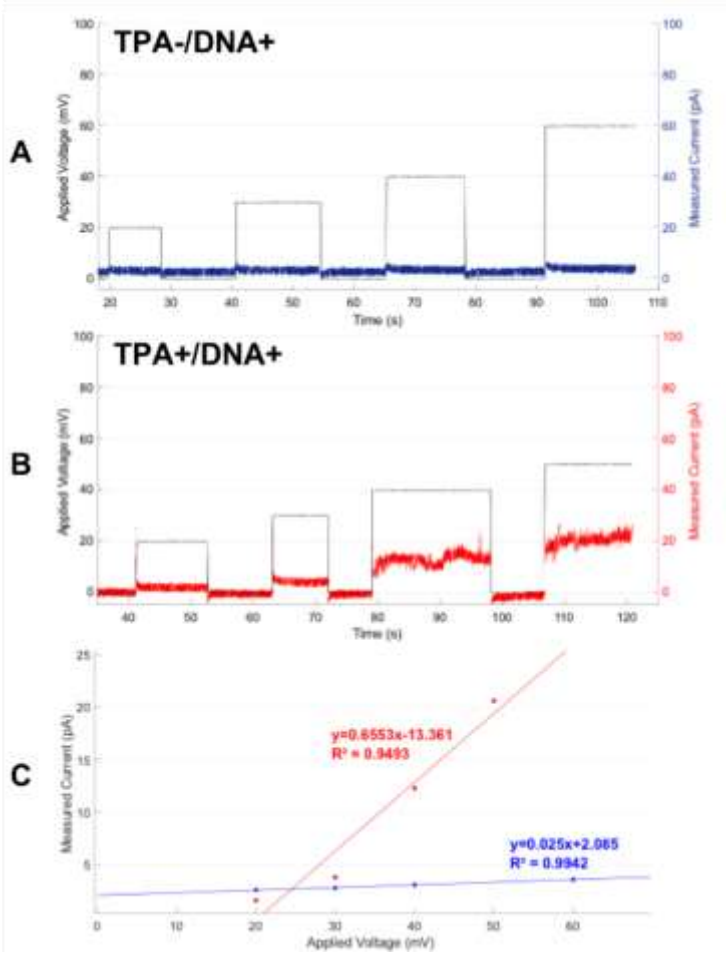

Figure 8. Current-voltage responses of membranes assembled between compartments containing the products of *in vitro* cell-free reactions.

(A) With DNA (JF001A) but without TPA (trigger) results in a highly resistive membrane that limits current induced by applied voltage.

(B) Current versus time for a bilayer formed from droplets containing the products of a reaction with both DNA and TPA included.

(C) Average current versus voltage for the data in A and B

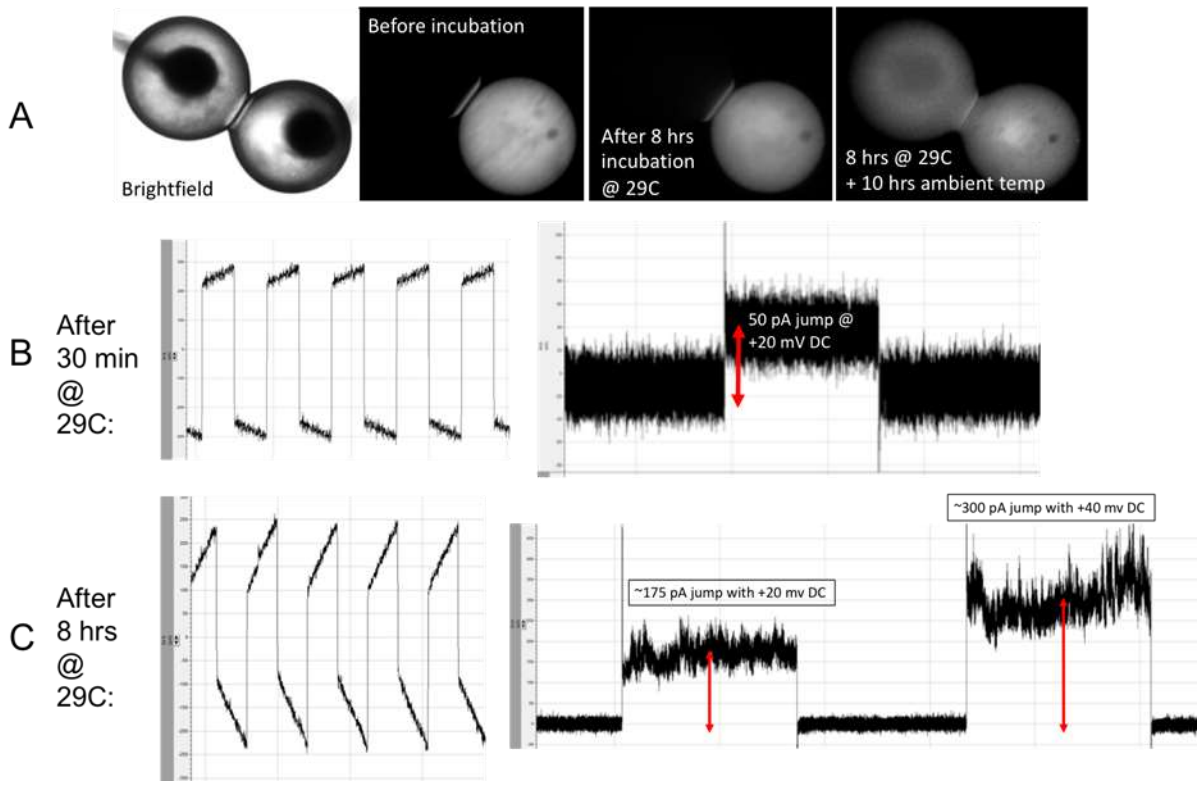

Figure 9. In situ, TPA-triggered synthesis of aHL and changes in membrane conductance

(A) Brightfield and fluorescence images of the two-compartment assembly.
(B) (B-C) AC (left) and DC (right) current measurements through the membrane.

These data show that initially both the current measurements and images demonstrate that the bilayer is resistance to ion transport and dye leakage between the droplets. However, as time passes, the amount of current passing through the bilayer increases and we observe that the fluorescence of the accepter droplet slowly grows. Again, these findings are consistent with the possibility that aHL synthesized within the droplets inserts into the membrane where it increases ion and dye permeability. However, given the disruptive properties of CFE it remains difficult to assess the number of channels in the membrane or quantitatively separate this outcome from non-specific permeation of the bilayer caused by the CFE.

6.0 SCHEDULE AND STATUS OF MILESTONES AND TASKS

Table 1. Summary of completed milestones

			Project Month									
Aim	**Task/Milestone**	**Description**	**1**	**2**	**3**	**4**	**5**	**6**	**7**	**8**	**9**	**Completion % (comments)**
1	Task 1.1	Develop and characterize Scheme 2 cassettes for sensing temperature shifts and producing actin and RFP proteins										Synthesized & tested 2 different temp.-sensitive switches (pCali2, mThermeleon)
	Milestone 1.1.1	Design/synthesize plasmids for 3 variants of Scheme 2, each which includes necessary expression promoter, RNA , and genes of interest sequences										100%
	Milestone 1.1.2	Confirm temperature-sensitive RNA thermometer functionality, and quantify RFP protein production kinetics and sensitivity										100%
	Milestone 1.1.3	Quantify actin protein production and sensitivity to temperature										100%
	Task 1.2	Develop and characterize Scheme 1 synthetic biology cassettes for sensing theophylline and producing alpha-hemolysin and GFP proteins										Synthesized & tested TP-sensitive riboswitch, demonstrated αHL + GFP production
	Milestone 1.2.1	Design/synthesize plasmids for 3 variants of Scheme 1, each which includes necessary expression promoter, RNA, and genes of interest sequences										100%
	Milestone 1.2.2	Confirm theophylline-sensitive riboswitch functionality, and quantify GFP protein production kinetics and sensitivity										100%
	Milestone 1.2.3	Quantify aHL protein production and sensitivity to TP										90% protein production scales with TP conc., minimum conc. not identified
	Task 1.3	Examine efficiency of Schemes 1 and 2 for orthogonal protein production when they are co-located in the same medium										successful orthogonal triggering of plasmids in same compartment.
	Milestone 1.3.1	Quantify actin and αHL protein production and their corresponding sensitivities to *theophylline* and temperature										90% quantities of each protein produced not obtained.
2	Task 2.1	Determine the effects of CFE machinery on material compartments										CFE disrupts lipid monolayer formation and bilayer stability; lipids in both oil and water help.
	Milestone 2.1.1	Assess the dynamic interfacial tension at oil-water interface of a compartment containing CFE										100%
	Milestone 2.1.2	Assess thickness, conductivity, and rupture potential of DIB membranes										100%
	Task 2.2	Determine the effects of non-triggered actin production and polymerization on compartment shape and membrane stability										Effects on droplet interface and bilayer understood
	Milestone 2.2.1	Micrographs and droplet shape information for isolated compartments										100%
	Milestone 2.2.2	Assess thickness, conductivity, and rupture potential of DIB membranes										100%
	Task 2.3	Analyze theophylline transport through an oil-based external medium into compartments for triggering material response										Will use αHL+GFP plasmid to assess TP transport via fluorescence
	Milestone 2.3.1	Determine the diffusion rate of *theophylline* in SEBS layer and the resulting sensing time lag in the compartment										100% TPB diffuses from oil to aqueous phases passively; no detectable lag in protein production
	Task 2.4	Characterize actin network structuring within the compartments, and analyze the change in modulus of the material in response to *temperature*										Demonstrated compatibility between CFE rxn and actin polymerization
	Milestone 2.4.1	Confocal micrographs of polymerized actin networks within compartments										20% (plan known, reaction verified, but not completed)
	Milestone 2.4.2	Measurements of compartment and material-level stiffness changes versus the amount of actin										50% successfully increased stiffness by *in situ* actin production/polymerization. Quantitative measures of stiffness not obtained.
3	Task 3.1	Demonstrate and assess change in DIB conductance upon non-triggered translation of αHL										Evidence of αHL insertion produced by CFE rxn
	Milestone 3.1.1	Demonstrate αHL channel insertion via cell-free translation										50% multiple experiments demonstrating higher membrane conductance when aHL could be synthesized.
	Milestone 3.1.2	Assess number, insertion kinetics, and unit conductance of αHL channels produced by non-triggered translation reactions										25%
	Task 3.2	Quantify biophysical changes in lipid-only membranes across temperature range of detection by RNA thermometer in absence of αHL										
	Milestone 3.2.1	Determine thickness, conductivity, and rupture potential of inter-compartmental membranes from 20-40°C										50% (not completed, lower priority)
	Task 3.3	Measure sensitivity between membrane conductance and *theophylline concentration*										0% unable to determine number of aHL present in the membrane
	Milestone 3.3.1	Determine dynamic and steady-state changes in conductance versus external theophylline dosing/concentration										0%
	Task 3.4	Predict and assess changes in conductivity of multicompartment material assemblies										
	Milestone 3.4.1	Develop a network model for multi-directional conductivity through compartmentalized materials										90%
	Milestone 3.4.2	Measure conductivity/transport of small molecules in 2D and 3D array of compartments										0%

* Milestones with less than 50% completion are highlighted in yellow.

7.0 REFERENCES

1. Aufinger, L.; Simmel, F. C., Artificial Gel-Based Organelles for Spatial Organization of Cell-Free Gene Expression Reactions. *Angewandte Chemie International Edition* **2018,** *57* (52), 17245-17248.
2. Zhou, X.; Wu, H.; Cui, M.; Lai, S. N.; Zheng, B., Long-lived protein expression in hydrogel particles: towards artificial cells. *Chemical Science* **2018,** *9* (18), 4275-4279.
3. Needham, D.; Kim, D. H., PEG-covered lipid surfaces: bilayers and monolayers. *Colloids and Surfaces B: Biointerfaces* **2000,** *18* (3-4), 183-195.
4. Needham, D.; Nunn, R. S., Elastic deformation and failure of lipid bilayer membranes containing cholesterol. *Biophys. J.* **1990,** *58* (4), 997-1009.
5. Lee, S.; Kim, D. H.; Needham, D., Equilibrium and Dynamic Interfacial Tension Measurements at Microscopic Interfaces Using a Micropipet Technique. 1. A New Method for Determination of Interfacial Tension. *Langmuir* **2001,** *17* (18), 5537-5543.

LIST OF SYMBOLS, ABBREVIATIONS, AND ACRONYMS

AFRL	Air Force Research Laboratory
aHL	Alpha-hemolysin
CFE	Cell-Free extract
DARPA	Defense Advanced Research Projects Agency
RFP	Red Fluorescent Protein
RXAP	Photonic Materials Branch, Functional Materials Division, Materials and Manufacturing Directorate of AFRL
TP	Theophylline
TPA	Theophylline Acetate
TPB	Tert-Butyl-Theophyllinate